Published in final edited form as:
Cancer Res. 2012 October 1; 72(19): 5080–5090. doi:10.1158/0008-5472.CAN-12-1484.

RAP80 is Critical in Maintaining Genomic Stability and Suppressing Tumor Development

Zhengyu Yin[1], **Daniel Menendez**[2], **Michael A. Resnick**[2], **John E. French**[3], **Kyathanahalli S. Janardhan**[4], and **Anton M. Jetten**[1,*]

[1]Laboratory of Respiratory Biology, National Institutes of Health, Research Triangle Park, NC 27909

[2]Laboratory of Molecular Genetics, National Institutes of Health, Research Triangle Park, NC 27909

[3]National Toxicology Program, National Institute of Environmental Sciences, National Institutes of Health, Research Triangle Park, NC 27909

[4]Integrated Laboratory Systems, Inc., National Institutes of Health, Research Triangle Park, NC 27909

Abstract

The ubiquitin interaction motif (UIM)-containing protein RAP80 was recently found to play a key role in DNA damage response (DDR) signaling by facilitating the translocation of several DDR mediators, including BRCA1, to ionizing irradiation (IR)-induced foci (IRIF). In this study, we examine the effect of the loss of RAP80 on genomic stability and the susceptibility to cancer development in RAP80 null ($RAP80^{-/-}$) mice. $RAP80^{-/-}$ mice are viable and did not exhibit any apparent developmental defects. Mouse embryonic fibroblasts (MEFs) derived from $RAP80^{-/-}$ mice underwent premature senescence compared to wild type (WT) MEFs, were more sensitive to IR, and exhibited a higher level of spontaneous and IR-induced genomic instability. $RAP80^{-/-}$ thymocytes were more sensitive to IR-induced cell death than WT thymocytes. $RAP80^{-/-}$ mice were more susceptible to spontaneous lymphoma development and the development of DMBA-induced mammary gland tumors. Moreover, the loss of RAP80 accelerated tumor formation in both $p53^{-/-}$ and $p53^{+/-}$ mice. Our data indicate that RAP80-deficiency promotes genomic instability and causes an increase in cancer risk consistent with the concept that RAP80 exhibits a tumor suppressor function.

Keywords

RAP80; UIMC1; Ubiquitin Interacting Motif; DNA repair; Trp53; mammary cancer; lymphoma; DMBA

Introduction

A proper response to DNA damage is essential for maintaining genomic stability and to prevent the accumulation and transmission of damaged DNA during cell division (1). Among the different types of DNA damage, DNA double-strand breaks (DSBs) are the most detrimental to mammalian cells. DSBs activate a DNA damage response (DDR) that

*To whom correspondence should be addressed. National Institute of Environmental Sciences, National Institutes of Health, 111 T.W. Alexander Drive, Research Triangle Park, NC 27709, jetten@niehs.nih.gov.

None of the authors state a conflict of interest.

coordinates the activation of cell cycle checkpoints, apoptosis, and DNA repair networks, to ensure accurate repair and genomic integrity. Defects in DNA repair mechanisms are associated with various human developmental and immune disorders and an increased cancer risk (2–5).

The DDR is initiated by sensors, such as the Mre11-Rad50-Nbs1 (MRN) complex, that detect DSBs and recruit effectors that carry out the repair, and mediators that promote the interactions between effectors and sensors (1, 6–9). At an early stage, the MRN recruits the ATM kinase, which upon activation catalyzes the phosphorylation of many proteins, including the histone variant H2AX (γH2AX), and promotes the recruitment and phosphorylation of MDC1 (1, 6–8, 10). Interaction of MDC1 with RING-finger ubiquitin ligase RNF8 and the subsequent association with the E2 ubiquitin-conjugating enzyme Ubc13 leads to the K63- or K6-linked polyubiquitylation of histones H2AX and H2A at the chromatin flanking DSBs, thereby amplifying the DSBs signals. The accumulation of DDR protein complexes at the break sites results in the formation of distinctive nuclear foci (ionizing radiation (IR)-induced foci or IRIF) (11, 12).

Receptor-Associated Protein 80 (RAP80 or UIMC1) is a Ubiquitin Interaction Motif-containing (UIMC) nuclear protein that is associated with several proteins, including BRCA1 (13–19), MDC1 (20), p53 (18), and the estrogen receptor alpha (ERα) (13). RAP80 facilitates the recruitment of the BRCA1-BARD1-Abraxas/CCDC98-MERIT-BRCC36 complex to IRIF. This translocation is mediated at least in part by the interaction of the UIMs of RAP80 to K63-linked polyubiquitin chains in histones at or near DSBs (11, 12). Cells in which RAP80 is knocked-down by siRNA, are impaired in forming and retaining IRIF containing BRCA1 and other downstream DDR proteins. These cells also exhibit increased radiosensitivity and impaired cell cycle checkpoints. In addition to its link with BRCA1, RAP80 was shown to be directly regulated by p53 and found to be associated with p53 in complex with E3 ubiquitin ligase HDM2 protein (18).

Its role in DDR and the potential link between *RAP80* mutations and human mammary and ovarian cancer, suggested that defective RAP80 function/expression might result in genomic instability and increased cancer risk (5, 21). In this study, we investigated the effect of the loss of RAP80 expression on genomic stability and cancer development in RAP80$^{-/-}$ mice using several tumorigenesis models, including IR-induced lymphoma and 7,12-dimethylbenz(a)anthracene (DMBA)-induced mammary cancer. Our results demonstrated that RAP80 protects against genomic instability and reduces cancer risk supporting the hypothesis that RAP80 functions as a tumor suppressor.

Material and Methods

Generation of RAP80 null Mice

RAP80$^{fx/fx}$ (B6(C)-Uimc$^{tm1.1Amj}$) and *RAP80* null mice (B6(C)-Uimc1$^{tm1.1Amj}$, referred to as RAP80$^{-/-}$) were generated as described in Supplemental Information and Fig. 1A and B.

Tumorigenesis studies

The formation of spontaneous tumors was monitored in male and female WT and RAP80$^{-/-}$ mice for a period of 20 months. For chemically induced tumor formation, 2 months old female WT and RAP80$^{-/-}$ mice were treated by gavage with DMBA (5 mg/ml in sesame oil; 1 mg/25 g total body weight; Sigma) once per week for 4 weeks and the development of mammary gland tumor formation and other tumors was monitored by weekly palpation for a period of 10 months (22). At 10 months, all mice were euthanized and necropsy performed to examine the presence of additional tumors. To determine the effect of the loss of RAP80 in p53-deficient mice, RAP80$^{-/-}$ mice were crossed with B6.129S2-Trp53^{tm1Tyj}/J (p53$^{+/-}$)

mice (The Jackson Laboratory) to generate RAP80$^{-/-}$ p53$^{+/-}$ and RAP80$^{-/-}$ p53$^{-/-}$ mice. Spontaneous and IR-induced tumor development was monitored and tumor-free survival analyzed by the Kaplan-Meier method using Graphpad Prism software.

In vitro MEF proliferation assays

RAP80$^{-/-}$ and *WT* MEFs were generated according to standard procedures (23). For the *in vitro* proliferation assay, 2×10^5 passage 1 MEFs were seeded onto each 60 mm dishes containing DMEM and 10% FBS and then incubated at 37°C under 5% CO_2. After 3–5 days upon confluence, the cells were trypsinized, counted, and reseeded at the same density of 3×10^5 cells/6-cm dish. Given two measurements of a growing quantity, q_1 at time t_1 and q_2 at time t_2, doubling time (Td) can be calculated with the following formula, $Td = (t_2 - t_1) * \log (2 - q_2/q_1)$. To measure actively proliferating cells, MEFs at various passages were pulse-labeled with 10 mM BrdU. After fixation cells were incubated with a biotinylated anti-BrdU antibody, and subsequently with a streptavidin-horseradish peroxidase-coupled secondary antibody and diaminobenzidine. Cells were counterstained with Harris hematoxylin (blue staining). Immortalized MEFs (iMEFs) were generated by SV40 T-antigen viral expression as described (24).

Immunofluorescence

Passage 3 MEFs or iMEFs derived from WT and RAP80$^{-/-}$ littermates were seeded onto coverslips and either left untreated or subjected to 4 or 10 Gy of γ radiation. At various time points after IR, the MEFs were fixed with 4% paraformaldehyde, permeabilized in 0.2% Triton X-100, and blocked in Superblock blocking buffer (Piece), followed by staining with rabbit anti-BRCA1 (kind gift from Dr. R Hakem, University of Toronto) and mouse monoclonal anti-γH2AX (Ser139; Upstate). Endogenous RAP80Ser205^P was detected with the RAP80Ser205^P antibody, prescribed previously (25). Donkey anti-mouse Alexa Fluor 595 and donkey anti-rabbit Alexa Fluor 488 (Invitrogen) were used for the secondary staining, followed by DAPI (Invitrogen) counterstaining. Images were taken on a laser confocal microscope (LSM510; Carl Zeiss, Inc.) under 40X or 60X magnification. For nuclear fragmentation assay, iMEFs were subjected to 4 Gy of γ radiation. Forty-eight hours later, 200 DAPI stained nuclei were counted for each genotype.

Protein analysis

WT or RAP80$^{-/-}$ iMEFs were either left untreated or subjected to 10 Gy of γ irradiation. At 10 min and 2 h after IR, cell lysates were collected and analyzed by SDS PAGE. The resolving bands were then transferred to PVDF membranes. Western blot analysis was performed using rabbit RAP80Ser205^P (25) and anti-GAPDH (Cell Signaling Technology) antibodies.

Colony-forming assay and β-galactosidase staining

iMEFs were seeded on 60-mm culture dishes (3×10^3 cells/dish). Cultures were either left untreated or subjected to various doses of γ radiation or UV and incubated for 14 days at 37°C. Cells were then stained with 1% Coomassie brilliant blue, 5% acetic acid, and 30% methanol and the number of colonies was counted. Senescence-associated (SA-β-gal) staining of MEFs was performed according to the manufacturer's protocol (BioVision).

Cell cycle analysis

MEFs or iMEFs were either left untreated or treated with various doses of γ radiation. At 24 h or 48h after radiation, cells were lifted by trypsin treatment and fixed in ice cold 70% ethanol before store in −20°C for overnight. Cells were then washed once with ice cold PBS

and stained with PI for 30 min before subject to Facsort to determine the DNA content. Cell cycle percentages were analyzed using Modfit software (Verity).

Sensitivity to IR and chemical stressors

MEFs, iMEFs or thymocytes ($0.5–1 \times 10^6$/ml in RPMI medium supplemented with 10% FCS and 5×10^{-5} M β-mercaptoethanol) were either left untreated or subjected to γ or UV radiation, or treated with doxorubicin, 5-fluorouracil, or nutlin-3a (Sigma) at the doses indicated (18). After 18 h, the number of apoptotic cells was determined using an Annexin-V-FITC/PI Apoptosis Detection Kit (BD Biosciences) following the manufacturer's protocol. QRT-PCR analysis of Bax, Puma, p21, Siva1, and Gapdh mRNA was performed as described in Supplemental Information. To assess radiosensitivity *in vivo*, 20 pairs of age-matched WT and RAP80$^{-/-}$ littermates were subjected to IR (8 Gy). Mice were monitored daily for survival and Kaplan-Meier survival curves were established. A log-rank test was used for statistical analysis.

Results

Generation and characterization of RAP80-null mice

To obtain greater insights into the physiological functions of RAP80, we generated *RAP80-null* mice by crossing RAP80$^{fx/fx}$ mice with Tg(CMV-Cre) mice as described in Supplemental Information and Fig. 1A and B. QRT-PCR showed that RAP80 mRNA expression was undetectable in testis, spleen and thymus, which normally express high levels of RAP80 (Fig. 1C). Western blot and immunofluorescence analysis showed that after IR treatment phosphorylated RAP80 was undetectable and did not accumulate at IRIFs in RAP80$^{-/-}$ MEFs consistent with the absence of RAP80 protein in these cells (Fig. 1D and E).

RAP80$^{-/-}$ mice exhibited a normal appearance and no anatomical or developmental defects were apparent. Deficiency in several DDR genes have been reported to affect spermatogenesis and to cause a reduction in the number of lymphocytes (26, 27); however, spermatogenesis appeared normal (data not shown) and both male and female RAP80$^{-/-}$ mice were fertile. FACS analysis showed little change in different CD4/CD8 thymocyte subpopulations between RAP80$^{-/-}$ and WT mice suggesting that loss of RAP80 did not affect thymopoiesis in a major way (data not shown).

Effect of RAP80 deficiency on senescence and radiosensitivity

The doubling time of RAP80$^{-/-}$ MEFs increased more rapidly upon passing than that of WT MEFs (Fig. 2A) and contained a lower number of bromodeoxyuridine (BrdU)-positive cells (Fig. 2B). By passage 3, RAP80$^{-/-}$ MEFs contained more non-dividing giant, β-gal positive senescent cells than WT cultures (Fig. S1A), suggesting that RAP80$^{-/-}$ MEFs underwent premature entry into senescence as was reported for mice deficient in other DDR genes, including BRCA1, Ku80, Ku70, and ATM (28, 29). Immortalized RAP80$^{-/-}$ and WT iMEFs no longer showed significant differences in proliferation and did not contain senescent cells (not shown). However, after UV irradiation, RAP80$^{-/-}$ iMEF cultures contained a larger number of senescent-like cells than those of WT iMEFs (Fig. S1B).

Because of its role in DDR, we examined whether the loss of RAP80 had any effect on radiosensitivity by examining the effect of IR on colony forming efficiency (CFE). Although at 2 and 4 Gy, IR reduced the CFE of RAP80$^{-/-}$ iMEFs to a greater extent than WT iMEFs, the differences were not statistically significant; however, at 6 Gy the reduction in CFE was significantly greater in RAP80$^{-/-}$ than WT iMEFs (Fig. 2C). Consistent with these observations, examination of the effect of IR on isolated thymocytes showed that RAP80$^{-/-}$

thymocytes were significantly more sensitive to IR-induced cell death than WT thymocytes (Fig. 2D). RAP80$^{-/-}$ mice exhibited a slightly greater susceptibility to whole body IR compared to WT littermates (Fig. S2); however, the difference was not statistically significant.

Effect of the loss of RAP80 on BRCA1 IRIF

Previous studies indicated that RAP80 facilitated the translocation of BRCA1 to IRIF (14–17). To further evaluate the effect of the loss of RAP80 on the localization of BRCA1 to IRIF, we compared the dynamics of BRCA1 foci formation in response to IR in WT or RAP80$^{-/-}$ MEFs. Although the loss of RAP80 did not prevent the formation of BRCA1 IRIF, a significant decrease in foci intensity and the percentage of cells containing nuclei with > 5 BRCA1^{+} foci was observed in RAP80$^{-/-}$ MEFs compared to WT MEFs 8 h after IR (Fig. 3A, B). This observation is consistent with a recent study showing that knockdown of RAP80 expression by siRNAs in U2OS cells did not prevent the formation of BRCA1 IRIF, but diminished the intensity of the foci and particularly reduced the retention of the foci at later time points (30).

Increased sensitivity of RAP80$^{-/-}$ MEFs to DNA damage agents and enhanced activation of p53-dependent pro-apoptotic pathways

Previously, we demonstrated that siRNA knockdown of RAP80 expression stabilizes p53 and results in increased transactivation of p53 target genes and increased apoptosis following DNA damage (18). We therefore determined whether RAP80$^{-/-}$ MEFs responded in a similar manner. Except for nutlin, which activates p53 by inhibiting its interaction with mdm2 without causing DNA damage, all treatments resulted in significantly more cell death in RAP80$^{-/-}$ MEFs than in WT MEFs (Fig. 4A). However, this difference in cell death was greatly reduced in WT and RAP80$^{-/-}$ iMEFs, which might be related to the inactivation of p53 by SV40 T-antigen (Fig. 4B). Moreover, IR, UV, doxorubicin and fluorouracil all increased the induction of the p53 target genes, Bax, Siva1 and Puma, to a greater extent in RAP80$^{-/-}$ MEFs than in WT MEFs, while the induction of these genes by nutlin was not significantly different between RAP80$^{-/-}$ and WT MEFs (Fig. 4C, Fig. S3). Little difference was observed in p21 expression.

Loss of RAP80 leads to prolonged G2/M cell cycle arrest upon DNA damage

Regulation of cell-cycle checkpoints is an integral part of the DDR (1, 9, 31, 32). Irradiation-induced checkpoints are activated during the G1 to S transition, the S phase, and the G2/M cell cycle boundary. To determine whether the loss of RAP80 affected cell cycle checkpoints, we compared the cell cycle distribution of RAP80$^{-/-}$ and WT MEFs in response to IR. At 24 h after exposure to 4 Gy IR, both WT and RAP80$^{-/-}$ MEFs exhibited a marked increase in the percentage of cells in G2/M, consistent with a G2/M arrest (Fig. 4D). At 48 h after IR, the percentage of WT MEFs in G2/M decreased, whereas that of RAP80$^{-/-}$ MEFs remained elevated. The prolonged G2/M arrest could be explained by the hypothesis that repair of DNA damage is less efficient in RAP80$^{-/-}$ MEFs.

RAP80 suppresses spontaneous and IR-induced genomic instability

Premature senescence observed in MEFs deficient in H2AX, ATM or BRCA1 expression has been reported to be associated with chromosomal instability (1, 3, 28, 33). Phosphorylation of H2AX (γH2AX) is thought to be a reliable indicator for DNA damage and genomic instability (2, 34). To examine the effect of the loss of RAP80 on genomic stability, we compared the number of γ-H2AX positive cells in untreated RAP80$^{-/-}$ and WT MEFs Under basal and low stress conditions RAP80$^{-/-}$ MEFs contained a significant higher percentage of cells with γ-H2AX positive nuclei than WT MEFs (Fig. 5A). All RAP80$^{-/-}$

and WT MEFs were γ-H2AX positive upon 4 Gy IR exposure (Fig. 5A, B); however, the γ-H2AX foci persisted longer in RAP80$^{-/-}$ MEFs than in WT MEFs (Fig. 5C). In addition, at 24 hours after IR RAP80$^{-/-}$ MEFs exhibited a greater extent of nuclear fragmentation as well as more micronuclei compared to WT MEFs (Fig. 5D). These observations are consistent with our conclusion that genetic lesions are repaired less efficiently in RAP80$^{-/-}$ MEFs than in WT.

To further examine whether the loss of RAP80 expression resulted in genomic instability, we analyzed metaphase spreads prepared from RAP80$^{-/-}$ and WT iMEFs treated with 4 Gy IR. An increase in the number of sister chromatid exchanges was observed in RAP80$^{-/-}$ MEFs (Fig. S4A, B) consistent with studies examining the effect of RAP80 knockdown by siRNA on genome stability (21, 30).

RAP80$^{-/-}$ mice exhibit an increased risk for spontaneous and IR-induced lymphomas

Mice deficient in several DDR proteins have been reported to exhibit an increased susceptibility to cancer development due to increased genomic instability (2, 35, 36). Because the loss of RAP80 expression results in less efficient DNA damage repair and enhanced genome instability, it has been suggested that it might influence cancer risk as well. We therefore monitored WT and RAP80$^{-/-}$ mice for over 20 months for spontaneous tumor formation. During the first 10 months, none of the WT or RAP80$^{-/-}$ mice developed tumors. However, by 20 months, 52% of the RAP80$^{-/-}$ mice had developed either thymic or splenic lymphomas, whereas only 1 out of 28 WT mice (3.6%) developed lymphoma (Fig. 6A). Occasionally, these lymphomas were found to infiltrate various non-lymphoid organs, including liver, lung, and kidney (Fig. S5A-F). In addition, RAP80$^{-/-}$ mice were more susceptible to IR-induced lymphoma formation. After exposure to 6 Gy IR, about 18% (4/22) of the RAP80$^{-/-}$ mice developed thymic lymphomas over a 6-month period, whereas only 4.7% (1/21) of the WT littermate controls did (Fig. 6B).

Loss of RAP80 accelerates tumor formation in p53$^{-/-}$ and p53$^{+/-}$ mice

Previous studies have shown that the loss of the tumor suppressor p53 greatly enhances tumor development in mice (35, 37). To determine whether the additional loss of RAP80 might further enhance tumor development in p53$^{-/-}$ mice, we examined tumor development in RAP80$^{-/-}$ p53$^{-/-}$ double-KO mice. RAP80$^{-/-}$ p53$^{-/-}$ mice did not show any developmental defects, but exhibited a significant decrease in tumor-free survival compared to p53$^{-/-}$ controls (Fig. 6A).

p53$^{+/-}$ mice have been reported to develop lymphomas and sarcomas at the age of 6–9 months and are widely used in short-term carcinogenicity testing (35, 37). To further examine the role of RAP80 in tumor development, we compared the susceptibility of RAP80$^{-/-}$, p53$^{+/-}$ RAP80$^{-/-}$, and p53$^{+/-}$ mice to IR-induced lymphoma formation. Although 42.8% (6/14) of p53$^{+/-}$ mice developed thymic lymphomas over a 4-month period, 78.5% (11/14) of p53$^{+/-}$ RAP80$^{-/-}$ developed thymic lymphomas (Fig. 6C). In addition, the average tumor weight of thymic lymphomas in p53$^{+/-}$ RAP80$^{-/-}$ mice was significantly greater than that of p53$^{+/-}$ mice (Fig. 6D). These results further support our conclusion that RAP80 deficiency enhances lymphoma development.

RAP80$^{-/-}$ mice exhibit an increased susceptibility to DMBA-induced mammary gland tumor development

We next compared the susceptibility of RAP80$^{-/-}$ and WT mice to DMBA-induced tumor formation. DMBA has been reported to induce the development of mammary gland and ovarian carcinomas, as well as lymphomas (22, 38). In our study, female WT and RAP80$^{-/-}$ mice were treated with DMBA once per week for 4 weeks and the development of

mammary gland tumor formation was monitored by weekly palpation for a period of 10 months. Over a period of 10 months only 5% of the WT mice developed DMBA-induced mammary gland tumors, which is consistent with reports that the C57BL6 strain is generally resistant to the development of DMBA-induced mammary tumors. In contrast, 40% of RAP80$^{-/-}$ mice developed mammary gland tumors (Fig. 7A). These observations support our hypothesis that the loss of RAP80 function causes an increased risk of mammary cancer development. DMBA treatment also induced lymphomas and ovarian carcinomas in both WT and RAP80$^{-/-}$ mice; however, no statistically significant difference in frequency was observed between WT and RAP80$^{-/-}$ mice. The overall tumor-free survival remained significantly different between RAP80$^{-/-}$ and WT mice (Fig. 7B). Collectively, these observations indicate that a deficiency in RAP80 increases the susceptibility to spontaneous and environmental stress-induced tumor formation in agreement with the conclusion that RAP80 functions as a tumor suppressor.

Discussion

Previous reports demonstrated that RAP80 plays an important role in DDR signaling. RAP80 is part of a BRCA1 protein complex and facilitates the translocation of the complex to DSBs (13–19, 39). This translocation is at least in part mediated through the interaction of the UIMs of RAP80 with K63- and K6-linked ubiquitinated γH2AX and other histones. Recently, Hu, et al. (30) reported that knockdown of RAP80 by siRNAs affected the retention of BRCA1 at IRIF rather then the initial recruitment of this complex. Our results showing diminished retention of BRCA1 complexes at IRIF at later times after DNA damage in MEFs derived from RAP80$^{-/-}$ embryos is in agreement with these observations. It was suggested that RAP80 complexes contribute to a process that down-modulates BRCA1 homologous recombination function and thereby suppressing exaggerated BRCA1-driven HR (30). This was corroborated by observations showing that the down-regulation of RAP80 by siRNA or expression of a functionally deficient RAP80 mutant in U2OS cells result in a hyper-recombination phenotype accompanied by increased chromosomal abnormalities, the majority of which consist of sister chromatid breaks and sister chromatid exchange (21, 30). Our analysis of chromosome spreads of iMEFs from WT and RAP80$^{-/-}$ mice indicated that the number of sister chromatid exchanges was significantly increased in IR exposed RAP80$^{-/-}$ iMEFs (Fig. S3) and further supports a role for RAP80 in the down-modulation of homologous recombination functions of BRCA1.

We further demonstrated that MEFs derived from RAP80$^{-/-}$ embryos undergo premature senescence. Moreover, RAP80$^{-/-}$ MEFs as well as RAP80$^{-/-}$ thymocytes, exhibited an increased sensitivity to several DNA damaging agents indicative of a less efficient DDR. Interesting the sensitivity to DNA damaging agents was p53 dependent. In addition, cultures of non-irradiated RAP80$^{-/-}$ MEFs contained a higher number of cells with γH2AX foci compared to WT cells and an increase in CtIP and BACH1 foci has been reported in U2OS cells in which RAP80 is down-regulated (21, 30, 40). These observations would be consistent with more extensive end processing of spontaneous single and double strand breaks in RAP80-deficient cells and with the concept that loss of RAP80 function leads to deficient DSB repair and increased chromosome instability.

A major role of DDR proteins in mammalian cells is to maintain genomic integrity. Impairment of the DDR process results in genome instability and increased cancer risk. In this study, we examined whether the loss of RAP80 expression affected cancer risk in several different murine cancer models. Our data showed that by 20 months the percentage of spontaneously developing lymphomas in RAP80$^{-/-}$ mice was significantly greater than in WT mice (52% versus 3.6%, respectively). IR exposure accelerated lymphoma formation in both WT and RAP80$^{-/-}$ mice; however, RAP80$^{-/-}$ mice remained more susceptible. Similar

findings were recently reported by Wu *et al.* (41). These observations indicate that loss of RAP80 enhances the susceptibility to lymphoma development consistent with the hypothesis that RAP80 functions as tumor suppressor.

It is well established that p53 acts as a tumor suppressor and plays an important role in determining heritable cancer risk (31, 35, 42). Inactivation of p53 acts cooperatively with genetic alterations in other tumor suppressor or oncogenes to increase cancer risk (43). In this study, we showed that RAP80$^{-/-}$ p53$^{-/-}$ double knockout mice exhibited a greater decrease in tumor-free survival compared to p53$^{-/-}$ single knockout mice indicating that the loss of RAP80 acts synergistically with the loss of p53 in promoting spontaneous lymphoma development. No statistically significant difference was observed in tumor-free survival between irradiated p53$^{-/-}$ and RAP80$^{-/-}$ p53$^{-/-}$ mice, which is likely due to the very small latency in tumor development. Heterozygous p53 knockout mice also exhibit a predisposition for developing lymphoma, sarcoma, and carcinoma and exposure to IR considerably reduces the latency to tumor formation and survival (37). We showed that p53$^{+/-}$ RAP80$^{-/-}$ mice were significantly more susceptible to the development of IR-induced thymic lymphomas than p53$^{+/-}$ mice (78.5% versus 42.8%, respectively). These observations suggest that inactivating RAP80 and p53 mutations cooperate in promoting tumorigenesis. The latter is consistent with the concept that RAP80 functions as a tumor suppressor. In agreement with previous observations (18), we found that the ability of several p53 activators to induce cell death and the expression of p53 target genes was significantly enhanced in RAP80$^{-/-}$ MEFs. As proposed for its modulation of BRCA1 (30), RAP80 might suppress the ability of p53 to transactivate apoptotic target genes in the presence of DNA stress and damage signals thereby increasing the time to repair.

In humans, germline mutations in BRCA1 and BRCA2 account for 5–7% of familial breast cancers (10, 44). Because RAP80 is part of a BRCA1 complex, we were particularly interested in determining whether RAP80$^{-/-}$ mice were more susceptible to DMBA-induced mammary cancer development. We found that RAP80$^{-/-}$ mice were significantly more susceptible to DMBA-induced mammary cancer development than WT mice. In addition to mammary cancer, DMBA treatment also enhanced the formation of lymphomas and ovarian cancer. Our results show that total tumor-free survival was significantly reduced in RAP80$^{-/-}$ mice. These observations are consistent with our conclusion that loss of RAP80 enhances cancer risk. Several recent studies investigating an association between RAP80 mutations and breast cancer risk in humans reported that truncating mutations of the RAP80 gene are not associated with familial breast cancer, while RAP80 haplotype or rare missense mutations may be weakly or moderately associated with elevated risk of breast cancer (45–47). A separate study found an association between a RAP80 haplotype and elevated ovarian cancer risk (5). Screening of Finnish BRCA1/BRCA2 mutation-negative breast cancer families revealed the presence of several RAP80 variants (21); however, whether these are associated with increased cancer risk remains to be established. Overall these studies appear to indicate that the mutations identified within RAP80 to-date do not play a major role in increasing the risk of breast cancer. In summary, our study indicates that the loss of RAP80 enhances genome instability and increases the susceptibility to cancer development in several mouse models of human cancer. The impact of RAP80 on DNA repair and maintenance of genomic stability are consistent with the concept that RAP80 can function as a tumor suppressor.

Supplementary Material

Refer to Web version on PubMed Central for supplementary material.

Acknowledgments

The authors would like to thank Drs. Michael Fessler and Alex Merrick for providing the p53 KO mouse strain, Dr. Hong Soon Kang with qRT-PCR analysis, Laura Miller for her help with colony management and dosing the mice, and Grace Liao for her assistance with the genotyping. This research was supported by the Intramural Research Program of the National Institute of Environmental Health Sciences, the National Institutes of Health (Z01-ES-101586 to AMJ and Z01-ES065079 to MAR).

References

1. Lukas J, Lukas C, Bartek J. More than just a focus: The chromatin response to DNA damage and its role in genome integrity maintenance. Nat Cell Biol. 2011; 13:1161–9. [PubMed: 21968989]
2. Bohgaki T, Bohgaki M, Cardoso R, Panier S, Zeegers D, Li L, et al. Genomic instability, defective spermatogenesis, immunodeficiency, and cancer in a mouse model of the RIDDLE syndrome. PLoS Genet. 2011; 7:e1001381. [PubMed: 21552324]
3. McKinnon PJ, Caldecott KW. DNA strand break repair and human genetic disease. Annual review of genomics and human genetics. 2007; 8:37–55.
4. Moraes MC, Neto JB, Menck CF. DNA repair mechanisms protect our genome from carcinogenesis. Front Biosci. 2012; 17:1362–88. [PubMed: 22201809]
5. Rebbeck TR, Mitra N, Domchek SM, Wan F, Friebel TM, Tran TV, et al. Modification of BRCA1-Associated Breast and Ovarian Cancer Risk by BRCA1-Interacting Genes. Cancer Res. 2011; 71:5792–805. [PubMed: 21799032]
6. Polo SE, Jackson SP. Dynamics of DNA damage response proteins at DNA breaks: a focus on protein modifications. Genes Dev. 2011; 25:409–33. [PubMed: 21363960]
7. Yan J, Jetten AM. RAP80 and RNF8, key players in the recruitment of repair proteins to DNA damage sites. Cancer Lett. 2008; 271:179–90. [PubMed: 18550271]
8. Huen MS, Chen J. The DNA damage response pathways: at the crossroad of protein modifications. Cell Res. 2008; 18:8–16. [PubMed: 18087291]
9. Kastan MB, Bartek J. Cell-cycle checkpoints and cancer. Nature. 2004; 432:316–23. [PubMed: 15549093]
10. Roy R, Chun J, Powell SN. BRCA1 and BRCA2: different roles in a common pathway of genome protection. Nat Rev Cancer. 2012; 12:68–78. [PubMed: 22193408]
11. Bekker-Jensen S, Mailand N. Assembly and function of DNA double-strand break repair foci in mammalian cells. DNA Repair (Amst). 2010; 9:1219–28. [PubMed: 21035408]
12. Greenberg RA. Histone tails: Directing the chromatin response to DNA damage. FEBS Lett. 2011; 585:2883–90. [PubMed: 21621538]
13. Yan J, Kim YS, Yang XP, Albers M, Koegl M, Jetten AM. Ubiquitin-interaction motifs of RAP80 are critical in its regulation of estrogen receptor alpha. Nucleic Acids Res. 2007; 35:1673–86. [PubMed: 17311814]
14. Yan J, Kim YS, Yang XP, Li LP, Liao G, Xia F, et al. The ubiquitin-interacting motif containing protein RAP80 interacts with BRCA1 and functions in DNA damage repair response. Cancer Res. 2007; 67:6647–56. [PubMed: 17621610]
15. Liu Z, Wu J, Yu X. CCDC98 targets BRCA1 to DNA damage sites. Nat Struct Mol Biol. 2007; 14:716–20. [PubMed: 17643121]
16. Sobhian B, Shao G, Lilli DR, Culhane AC, Moreau LA, Xia B, et al. RAP80 targets BRCA1 to specific ubiquitin structures at DNA damage sites. Science. 2007; 316:1198–202. [PubMed: 17525341]
17. Wang B, Matsuoka S, Ballif BA, Zhang D, Smogorzewska A, Gygi SP, et al. Abraxas and RAP80 form a BRCA1 protein complex required for the DNA damage response. Science. 2007; 316:1194–8. [PubMed: 17525340]
18. Yan J, Menendez D, Yang XP, Resnick MA, Jetten AM. A regulatory loop composed of RAP80-HDM2-p53 provides RAP80-enhanced p53 degradation by HDM2 in response to DNA damage. J Biol Chem. 2009; 284:19280–9. [PubMed: 19433585]

19. Kim H, Chen J, Yu X. Ubiquitin-binding protein RAP80 mediates BRCA1-dependent DNA damage response. Science. 2007; 316:1202–5. [PubMed: 17525342]
20. Strauss C, Halevy T, Macarov M, Argaman L, Goldberg M. MDC1 is ubiquitylated on its tandem BRCT domain and directly binds RAP80 in a UBC13-dependent manner. DNA Repair (Amst). 2011; 10:806–14. [PubMed: 21622030]
21. Nikkila J, Coleman KA, Morrissey D, Pylkas K, Erkko H, Messick TE, et al. Familial breast cancer screening reveals an alteration in the RAP80 UIM domain that impairs DNA damage response function. Oncogene. 2009; 28:1843–52. [PubMed: 19305427]
22. Medina D, Butel JS, Socher SH, Miller FL. Mammary tumorigenesis in 7,12-dimethybenzanthracene-treated C57BL x DBA/2f F1 mice. Cancer Res. 1980; 40:368–73. [PubMed: 6243251]
23. McElroy SL, Reijo Pera RA. Preparation of mouse embryonic fibroblast feeder cells for human embryonic stem cell culture. CSH Protoc. 2008 2008:pdb prot5041.
24. Takeda Y, Kang HS, Angers M, Jetten AM. Retinoic acid-related orphan receptor gamma directly regulates neuronal PAS domain protein 2 transcription in vivo. Nucleic Acids Res. 2011; 39:4769–82. [PubMed: 21317191]
25. Yan JY, XP, Kim YS, Jetten AM. RAP80 responds to DNA damage induced by both ionizing radiation and UV irradiation and is phosphorylated at Ser205. Cancer Res. 2008; 68:4269–76. [PubMed: 18519686]
26. Lu LY, Wu J, Ye L, Gavrilina GB, Saunders TL, Yu X. RNF8-dependent histone modifications regulate nucleosome removal during spermatogenesis. Dev Cell. 2010; 18:371–84. [PubMed: 20153262]
27. Santos MA, Huen MS, Jankovic M, Chen HT, Lopez-Contreras AJ, Klein IA, et al. Class switching and meiotic defects in mice lacking the E3 ubiquitin ligase RNF8. J Exp Med. 2010; 207:973–81. [PubMed: 20385748]
28. Cao L, Li W, Kim S, Brodie SG, Deng CX. Senescence, aging, and malignant transformation mediated by p53 in mice lacking the Brca1 full-length isoform. Genes Dev. 2003; 17:201–13. [PubMed: 12533509]
29. Wang YA, Elson A, Leder P. Loss of p21 increases sensitivity to ionizing radiation and delays the onset of lymphoma in atm-deficient mice. Proc Natl Acad Sci U S A. 1997; 94:14590–5. [PubMed: 9405657]
30. Hu Y, Scully R, Sobhian B, Xie A, Shestakova E, Livingston DM. RAP80-directed tuning of BRCA1 homologous recombination function at ionizing radiation-induced nuclear foci. Genes Dev. 2011; 25:685–700. [PubMed: 21406551]
31. Levine AJ, Oren M. The first 30 years of p53: growing ever more complex. Nat Rev Cancer. 2009; 9:749–58. [PubMed: 19776744]
32. Toledo F, Wahl GM. Regulating the p53 pathway: in vitro hypotheses, in vivo veritas. Nat Rev Cancer. 2006; 6:909–23. [PubMed: 17128209]
33. Celeste A, Petersen S, Romanienko PJ, Fernandez-Capetillo O, Chen HT, Sedelnikova OA, et al. Genomic instability in mice lacking histone H2AX. Science. 2002; 296:922–7. [PubMed: 11934988]
34. Rogakou EP, Pilch DR, Orr AH, Ivanova VS, Bonner WM. DNA double-stranded breaks induce histone H2AX phosphorylation on serine 139. J Biol Chem. 1998; 273:5858–68. [PubMed: 9488723]
35. Donehower LA, Godley LA, Aldaz CM, Pyle R, Shi YP, Pinkel D, et al. The role of p53 loss in genomic instability and tumor progression in a murine mammary cancer model. Prog Clin Biol Res. 1996; 395:1–11. [PubMed: 8895979]
36. Narod SA, Foulkes WD. BRCA1 and BRCA2: 1994 and beyond. Nat Rev Cancer. 2004; 4:665–76. [PubMed: 15343273]
37. Backlund MG, Trasti SL, Backlund DC, Cressman VL, Godfrey V, Koller BH. Impact of ionizing radiation and genetic background on mammary tumorigenesis in p53-deficient mice. Cancer Res. 2001; 61:6577–82. [PubMed: 11522657]

38. Argov S, Cochran AJ, Karre K, Klein GO, Klein G. Incidence and type of tumors induced in C57BL bg/bg mice and +/bg littermates by oral administration of DMBA. Int J Cancer. 1981; 28:739–46. [PubMed: 6800966]
39. Shao G, Lilli DR, Patterson-Fortin J, Coleman KA, Morrissey DE, Greenberg RA. The Rap80-BRCC36 de-ubiquitinating enzyme complex antagonizes RNF8-Ubc13-dependent ubiquitination events at DNA double strand breaks. Proc Natl Acad Sci U S A. 2009; 106:3166–71. [PubMed: 19202061]
40. Coleman KA, Greenberg RA. The BRCA1-RAP80 complex regulates DNA repair mechanism utilization by restricting end resection. J Biol Chem. 2011; 286:13669–80. [PubMed: 21335604]
41. Wu J, Liu C, Chen J, Yu X. RAP80 Protein Is Important for Genomic Stability and Is Required for Stabilizing BRCA1-A Complex at DNA Damage Sites in Vivo. J Biol Chem. 2012; 287:22919–26. [PubMed: 22539352]
42. Chang F, Syrjanen S, Tervahauta A, Syrjanen K. Tumourigenesis associated with the p53 tumour suppressor gene. Br J Cancer. 1993; 68:653–61. [PubMed: 8398688]
43. McAllister KA, Houle CD, Malphurs J, Ward T, Collins NK, Gersch W, et al. Spontaneous and irradiation-induced tumor susceptibility in BRCA2 germline mutant mice and cooperative effects with a p53 germline mutation. Toxicol Pathol. 2006; 34:187–98. [PubMed: 16546942]
44. Hollestelle A, Wasielewski M, Martens JW, Schutte M. Discovering moderate-risk breast cancer susceptibility genes. Curr Opin Genet Dev. 2010; 20:268–76. [PubMed: 20346647]
45. Osorio A, Barroso A, Garcia MJ, Martinez-Delgado B, Urioste M, Benitez J. Evaluation of the BRCA1 interacting genes RAP80 and CCDC98 in familial breast cancer susceptibility. Breast Cancer Res Treat. 2009; 113:371–6. [PubMed: 18270812]
46. Novak DJ, Sabbaghian N, Maillet P, Chappuis PO, Foulkes WD, Tischkowitz M. Analysis of the genes coding for the BRCA1-interacting proteins, RAP80 and Abraxas (CCDC98), in high-risk, non-BRCA1/2, multiethnic breast cancer cases. Breast Cancer Res Treat. 2009; 117:453–9. [PubMed: 18695986]
47. Akbari MR, Ghadirian P, Robidoux A, Foumani M, Sun Y, Royer R, et al. Germline RAP80 mutations and susceptibility to breast cancer. Breast Cancer Res Treat. 2009; 113:377–81. [PubMed: 18306035]

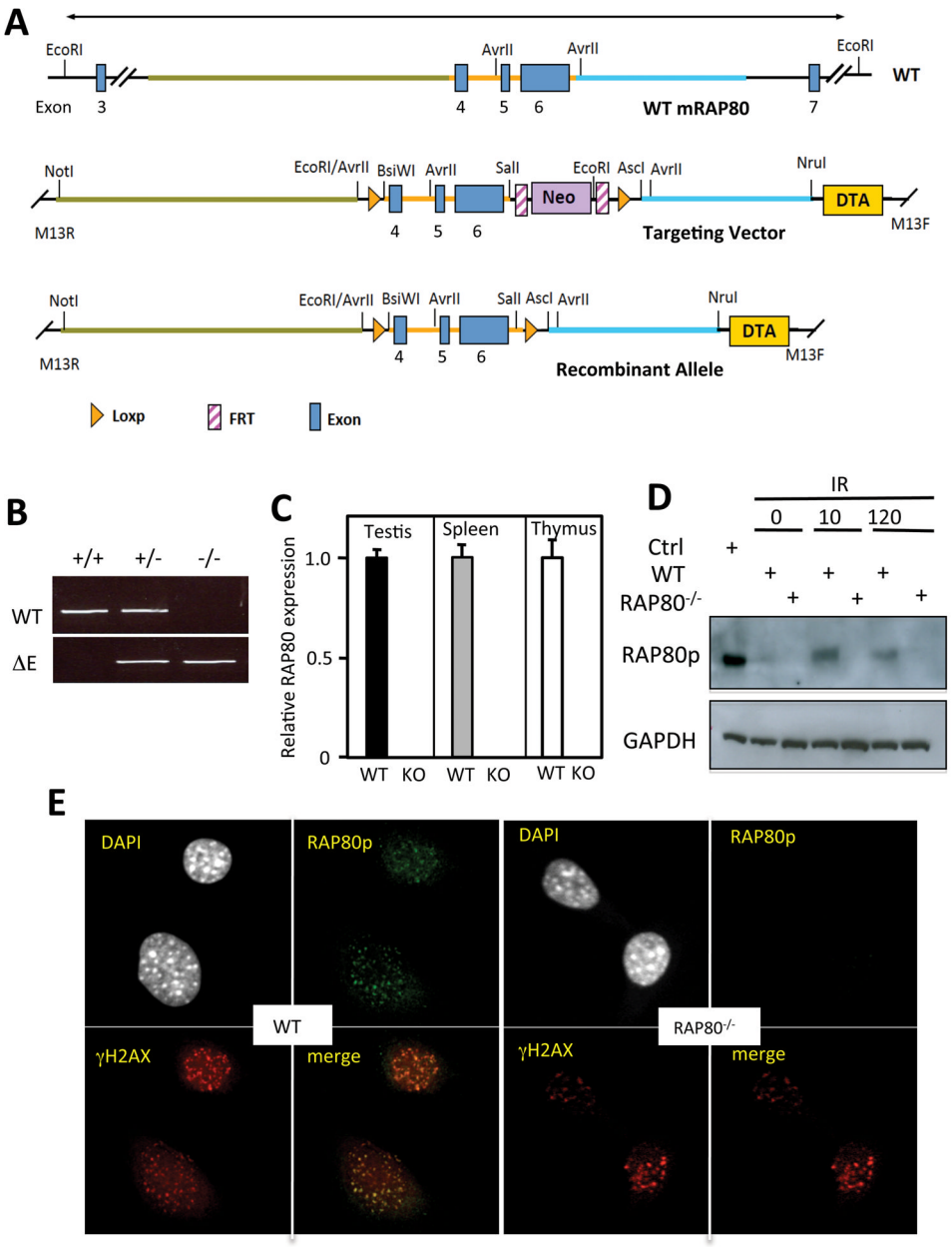

Figure 1.

Generation of RAP80 null Mice. (A) Strategy of generating RAP80 null mice. Schematic view of the mouse RAP80 locus, the targeting vector pLoxFtNwCD-RAP80, and the recombination at the RAP80 locus. LoxP and FRT sites are indicated. The RAP80fx/fx offspring were crossed with B6.C-Tg(CMV-cre)1Cgn/J to generate ubiquitous RAP80$^{-/-}$ mice. This results in the deletion of a ~2.5 kb region containing parts of introns 3 and 6, and exons 4–6 which encode the section between ^{79}Met and ^{367}Ser, including the two UIMs, and places exon 3 out of frame with exon 7. (B). PCR genotype analysis of WT and RAP80$^{-/-}$. WT and ΔE represent the WT and RAP80$^{-/-}$ recombinant alleles, respectively. (C) RAP80 mRNA expression in testis, spleen, and thymus from WT and RAP80$^{-/-}$ mice by QRT-PCR. (D) Untreated WT and RAP80$^{-/-}$ iMEFs or cells exposed to IR and 10 min or 2 h later cell lysates were collected and examined by Western blot analysis with RAP80Ser205^{P} and

GAPDH antibodies. (E) WT and RAP80$^{-/-}$ iMEFs were untreated or exposed to IR and four hours later examined by immunofluorescent staining with anti-γH2AX and anti-RAP80Ser205^{P} antibodies. Nuclei were counterstained with DAPI.

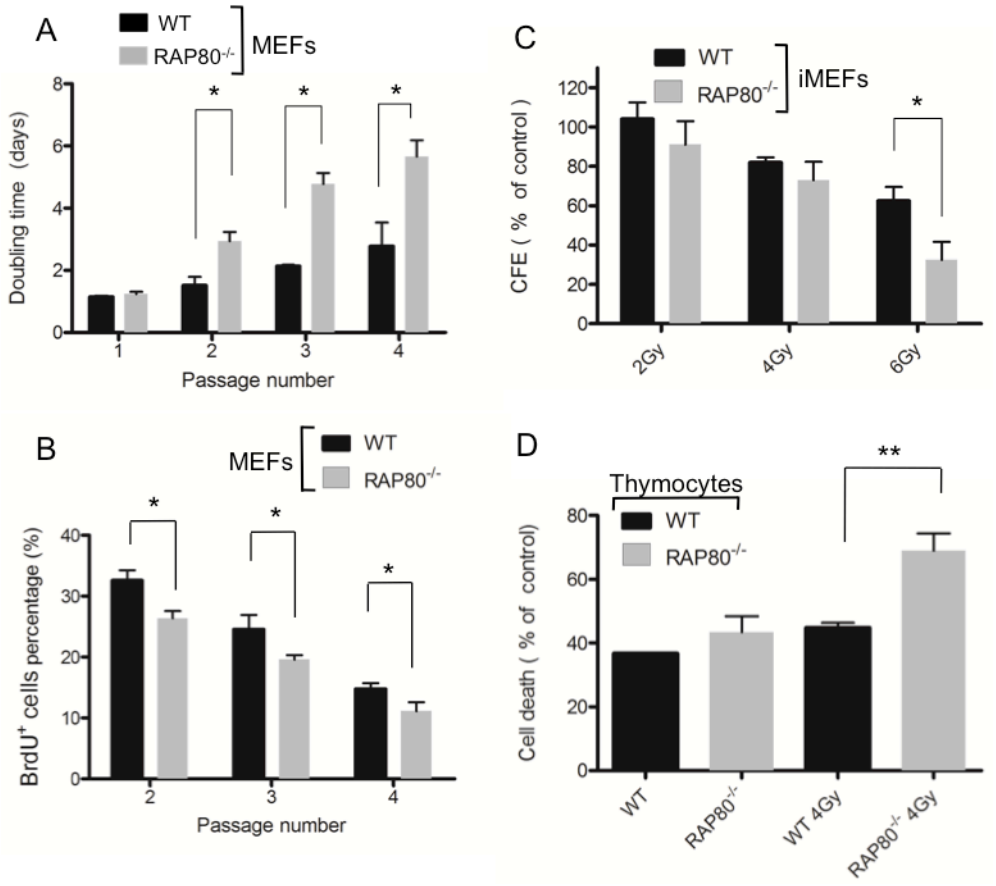

Figure 2.

RAP80 deficiency leads to early senescence and increased radiosensitivity. (A) Loss of RAP80 in MEFs caused a rapid increase in doubling time. (B) MEFs at various passages were pulse-labeled with BrdU and the percentage of BrdU-positive cells determined. (C) Untreated iMEFs or cells exposed to various doses of IR were incubated for 14 days at 37°C before colony forming efficiency (CFE) was determined. (D) Isolated thymocytes from WT and RAP80$^{-/-}$ mice were left untreated or irradiated at 4 Gy and cell viability was determined by PI staining. *, $p<0.05$; **, $p<0.01$.

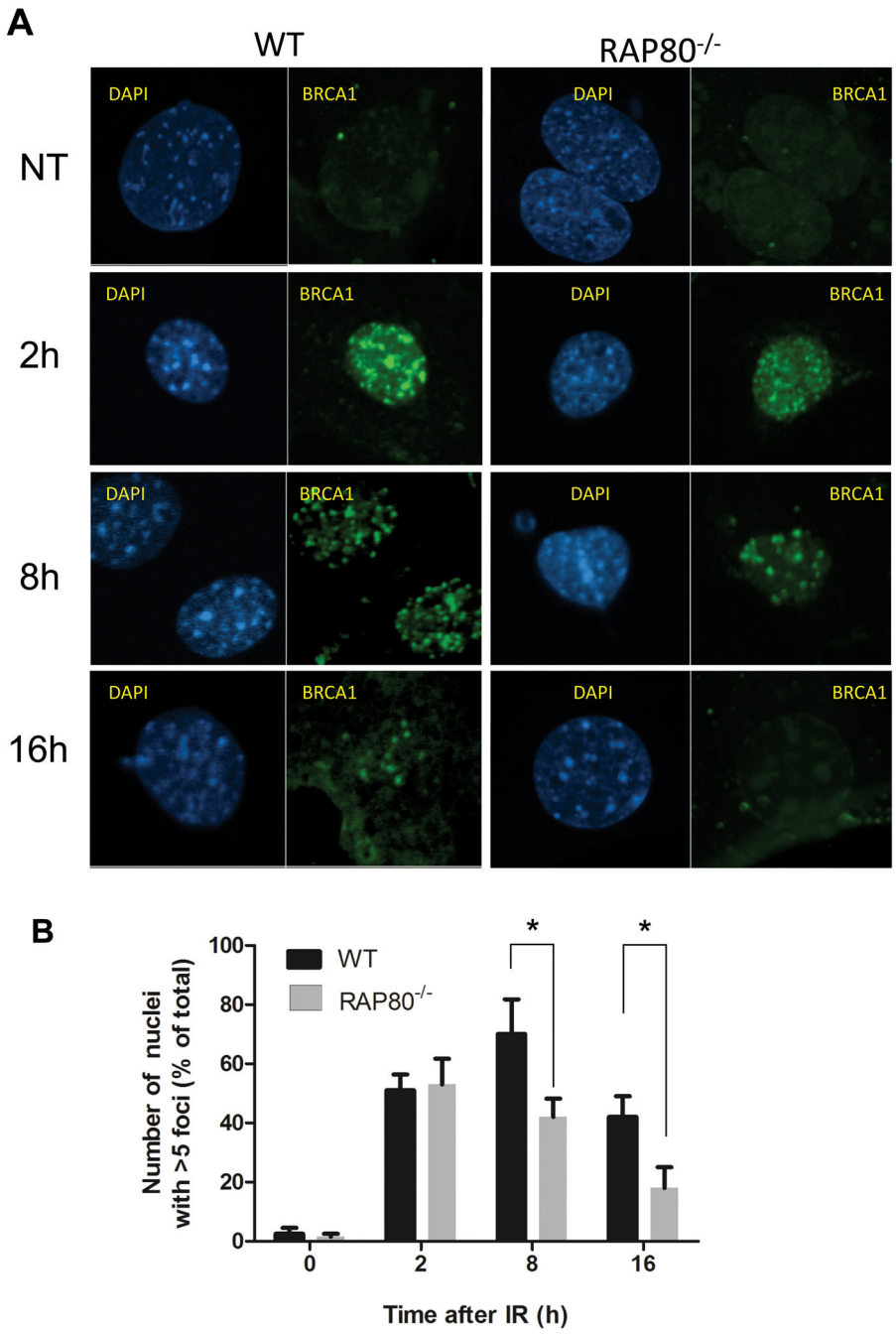

Figure 3.

BRCA1 IRIF formation. WT and RAP80$^{-/-}$ MEFs were irradiated with 4 Gy IR or mock-treated (designated as NT) and BRCA1 IRIF examined at different time points. (A) Representative images showing BRCA1 IRIF at 0, 2, 8 and 16 h post-IR. Nuclei were counterstained with DAPI. (B) At the indicated times the percentages of nuclei containing at least 5 distinct BRCA1 foci, were counted. At least 50 nuclei were counted at each time point. The experiment was repeated three times and error bars indicate standard deviation. Data were analyzed using two-way ANOVA. *, $p < 0.05$.

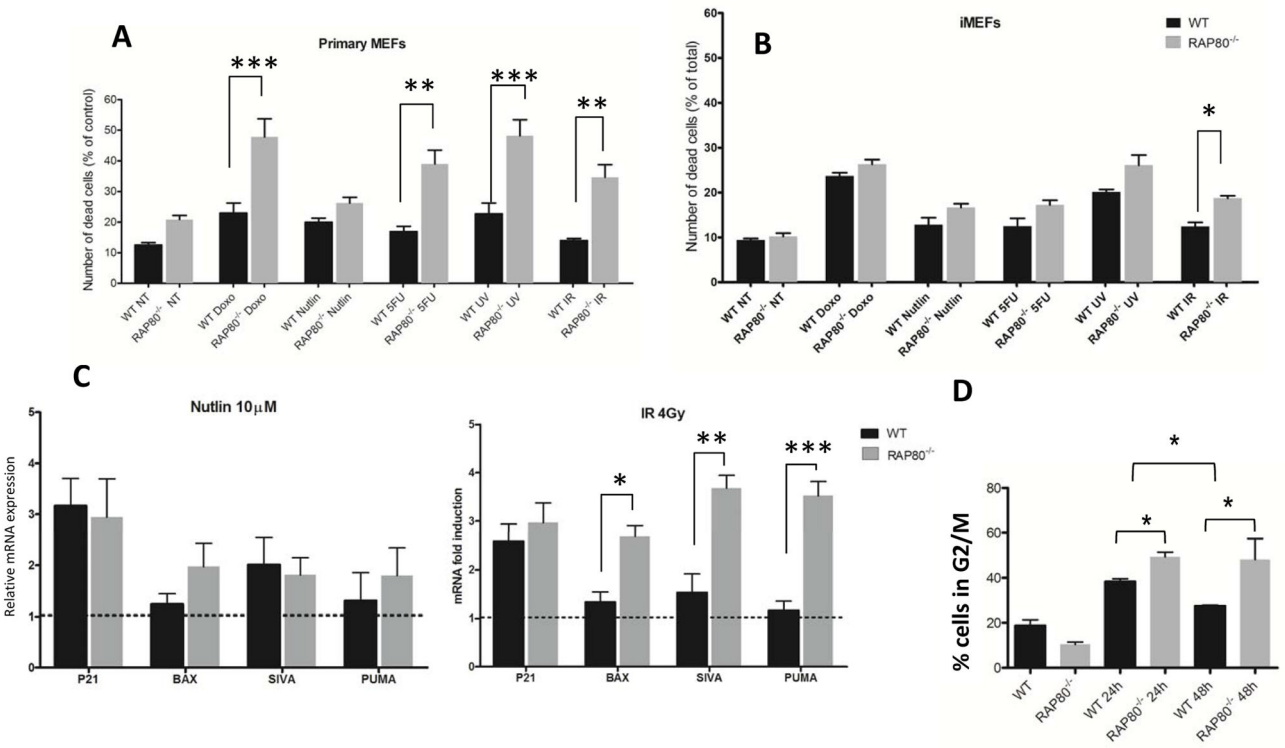

Figure 4.

Increased sensitivity of RAP80$^{-/-}$ MEFs to DNA damaging agents. WT and RAP80$^{-/-}$ MEFs (A, C) or iMEFs (B) were exposed to IR (4Gy) or treated with nutlin (10 μM). After 18 h, the percentage of apoptotic cells (A, B) or the expression of P21, BAX, SIVA and PUMA mRNA analyzed by qRT-PCR (C). (D) IR exposure induced an increased G2/M cell cycle arrest in RAP80$^{-/-}$ MEFs compared to WT MEFs. MEFs were either left untreated or treated with IR (4 Gy) and after 24 or 48 h stained with PI, analyzed by flow cytometry, and the percentage of cells in G2/M calculated. *, $p<0.05$; **, $p<0.01$; ***, $p<0.001$.

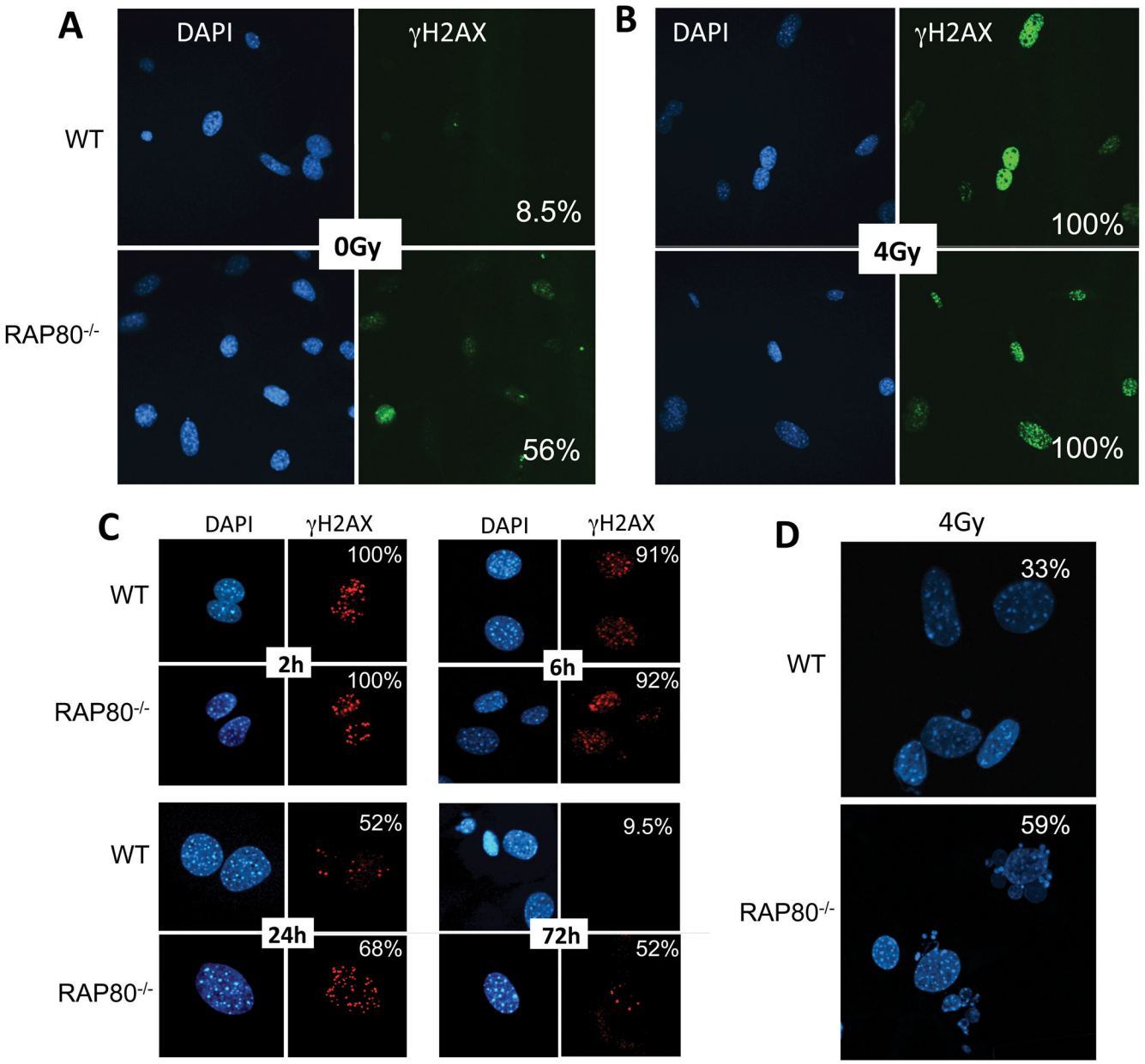

Figure 5.

RAP80 suppresses spontaneous and IR-induced genomic instability. (A, B) WT and RAP80$^{-/-}$ MEFs were γ-irradiated (4 Gy) and 2 h later stained with anti-γ-H2AX and DAPI. The percentage of cells containing γ-H2AX foci was determined. (C) IR-induced γ-H2AX foci are more persistent in RAP80$^{-/-}$ MEFs compared to WT MEFs. Percentages of γH2AX fluorescent cells are indicated. (D) WT and RAP80$^{-/-}$ MEFs were exposed to IR (4 Gy), 24 h later fixed, stained with DAPI, and the percentage of fragmented nuclei calculated (n = 200 nuclei).

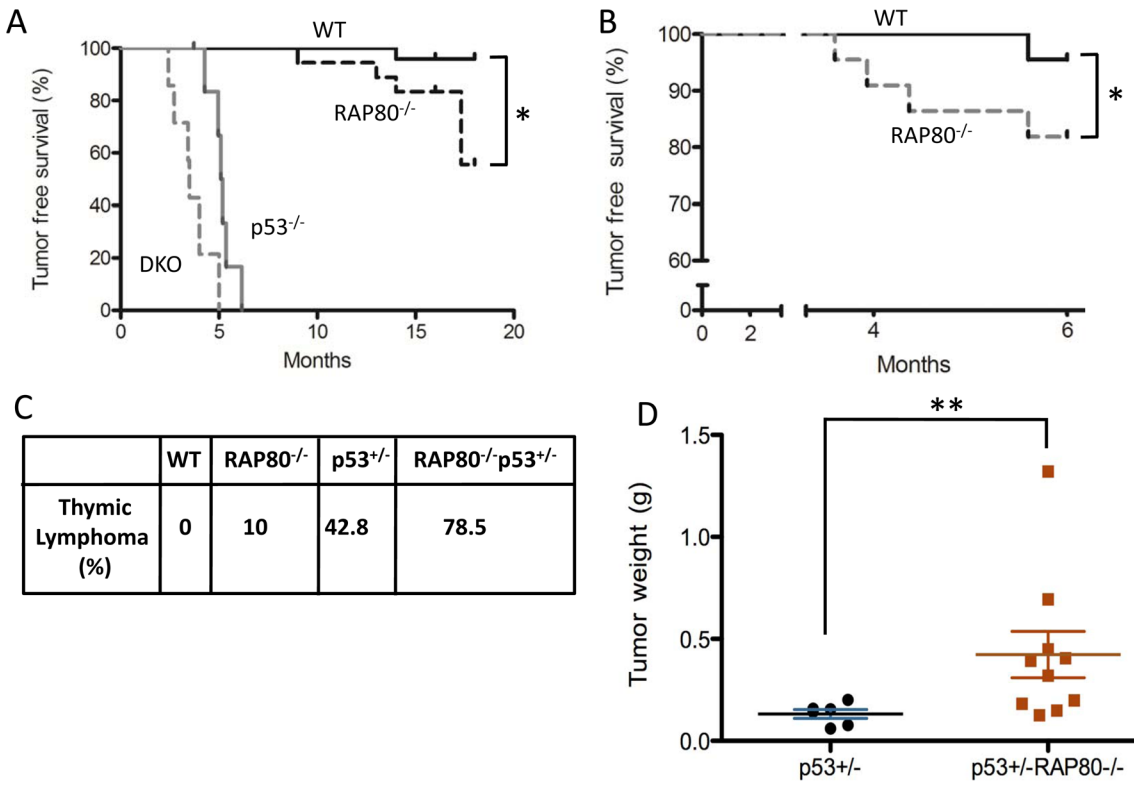

	WT	RAP80$^{-/-}$	p53$^{+/-}$	RAP80$^{-/-}$p53$^{+/-}$
Thymic Lymphoma (%)	0	10	42.8	78.5

Figure 6.

RAP80$^{-/-}$ mice exhibit an increased susceptibility to tumor formation. (A) WT, RAP80$^{-/-}$, p53$^{-/-}$, and RAP80$^{-/-}$ p53$^{-/-}$ (DKO) mice were monitored for the formation of spontaneous tumor formation and tumor-free survival analyzed by the Kaplan-Meier method. (B) WT and RAP80$^{-/-}$ mice (n=20) were exposed to 6 Gy IR. The development of IR-induced tumors in WT and RAP80$^{-/-}$ mice was closely monitored for 6 months. (C) WT, RAP80$^{-/-}$, p53$^{+/-}$, and p53$^{+/-}$ RAP80$^{-/-}$ mice (n=14–20) were exposed to 6 Gy IR and the percentage of mice with thymic lymphomas determined. (D) At 4 months the average tumor weight of thymic lymphomas in p53$^{+/-}$ RAP80$^{-/-}$ mice was significantly greater than that of p53$^{+/-}$ mice. *, p <0.05; **, p <0.01.

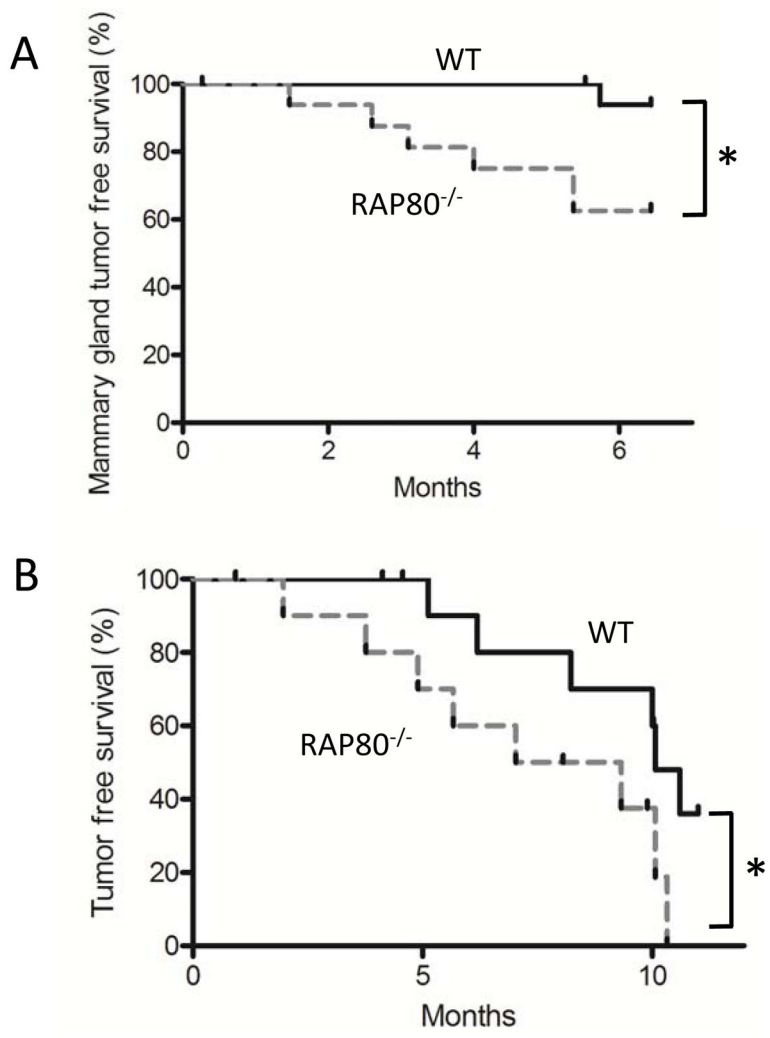

Figure 7.

RAP80$^{-/-}$ mice exhibit an increased susceptibility to DMBA-induced mammary gland tumor development. Female WT and RAP80$^{-/-}$ mice were treated with DMBA once per week for 4 weeks. Mammary gland tumor (A) and total tumor (B) development was monitored by weekly palpation. Kaplan-Meier survival curves were established. N=20. *, p <0.05.